Processing of polymer-derived silicon carbide foams and their adsorption capacity for non-steroidal anti-inflammatory drugs

(Article begins on next page)

15 October 2023

iris - AperTO

University of Turin's Institutional Research Information System and Open Access Institutional Repository

Processing of polymer-derived silicon carbide foams and their adsorption capacity for non-steroidal anti-inflammatory drugs

Prasanta Jana*[a], Maria Concetta Bruzzoniti[b], Marta Appendini[b], Luca Rivoira[b], Massimo Del Bubba[c], Daniele Rossini[c], Lorenzo Ciofi[c], Gian Domenico Sorarù[a]

[a]*Department of Industrial Engineering, University of Trento, Via Sommarive 9, 38123 Trento, Italy*

[b]*Department of Chemistry, University of Turin, Via P. Giuria 5, 10125 Turin, Italy*

[c]*Department of Chemistry "Ugo Schiff", University of Florence, Via della Lastruccia 3, 50019 Sesto Fiorentino, Italy*

Abstract

A process is described for preparing light weight and low cost polymer-derived silicon carbide foams by impregnation with polymeric precursor and polyurethane foam, followed by pyrolysis in inert atmosphere. Scanning electron microscopy showed that the resultant silicon carbide foams had a fully open and interconnected porous structure with dense struts. The suitability of these silicon carbide foams for the adsorption of non-steroidal anti-inflammatory drugs and their metabolites was studied. The results showed that silicon carbide foams adsorbed the target compounds and adsorption capacity increases with increasing the contact time between the foam and the analytes investigated.

*Corresponding author:

E-mail addresses: prasanta.jana@unitn.it

Telephone: +39461282454, Fax: +39461281977

1. Introduction

Risk of contamination of the environment from pharmaceuticals is increasing day-by-day. Over 200 different pharmaceutical agents, including antibiotics, non-steroidal anti-inflammatory drugs (NSAIDs), analgesics, lipid-lowering drugs, estrogens and drugs from other therapeutic groups, have been detected in aquatic and terrestrial environments around the world [1–6].

Most residential, industrial and agricultural wastewater containing pharmaceuticals eventually reach wastewater treatment plants (WWTPs) before discharging into water bodies. Most WWTPs are based on biological treatments and are not specifically designed to remove pharmaceuticals. Accordingly, drugs and their metabolites have been observed at concentrations ranging from part-per-trillion to part-per-billion levels in effluent wastewater [7, 8] and in sludge [9] from WWTPs treating various kinds of wastewater. Thus, inadequately treated municipal wastewater, as well as waste from hospitals, drug production facilities and livestock farming, are potential sources for ubiquitous occurrence of these pharmaceuticals in the environment, including rivers, lakes, and groundwater [10].

Various methods have been adopted so far for NSAIDs removal from drinking water or wastewater. Coagulation-flocculation, bio-degradation and photo-degradation, bio-filtration, ozonation, chlorination and adsorption [11–15] are some of the methods studied until now. Each processes has shortcomings with respect to high investment and maintenance costs, secondary pollution and complicated procedure involved in the treatment. For example, bio/photo-degradation can be effective for the removal of NSAIDs compounds. However, it can lead to the formation of undesirable byproducts, which can be even more dangerous than the precursor [16]. On the other hand, adsorption processes do not add undesired by-products and are superior to other techniques for wastewater treatment in terms of simplicity of design and operation. It should also be remarked that, in contrast to findings observed in biological processes, adsorption treatments are not affected by the presence of toxic substances in wastewater [16].

Among the various materials employed as adsorbents, activated carbon has been tested for the removal of different types of NSAIDs [16], showing better performances compared to other materials. Activated carbon is employed as powder or granular form, which in general requires a scaffold or a filter. Furthermore, after activated carbon has become exhausted, the

regeneration process results in a loss of carbon and the regenerated material has a lower adsorption efficiency, compared to the virgin product.

The use of a foam as adsorbing material has advantages and disadvantages: foams have in general lower surface area which may result into lower capacity, but at the same time foams can be used as a cartridge without the need of scaffold or a filter and their regeneration is simple and effective without loss of materials. Highly porous foams such as silicon carbide (SiC) foams presented in this study would also ensure a low pressure drop for effluents.

Specific advantages of the SiC foams reported in this study over many oxide-based ceramic materials are the exceptional thermal stability, high mechanical strength, excellent resistance to oxidation and corrosion, low coefficient of thermal expansion and high heat conductivity. Accordingly, SiC foams have been tested for a variety of applications, such as filters and membranes [17–20], catalytic supports [21, 22], high temperature structural materials [23, 24], porous burners [25–27] and solar energy collectors [28]. Furthermore, many industries have already exploited SiC foams in water filtration, porous burners or diesel particulate filters.

Different processing routes for porous SiC ceramic foams have been developed for specific applications to satisfy the associated requirements for porosity, pore size and degree of interconnectivity. The processes can be divided into five categories: (i) partial sintering, (ii) replica, (iii) sacrificial template, (iv) direct foaming and (v) bonding techniques. Each fabrication method is suited for producing a specific range of pore sizes and overall amount of porosity. Most methods require many steps, are time consuming and not so cost effective for preparing SiC foams [29, 30].

Polymer derived ceramics (PDCs) are nanostructured ceramic materials obtained through pyrolysis of polymer precursors, under controlled atmosphere. PDCs have enabled significant technological breakthroughs in ceramic science and technology, also providing a route to new multifunctional ceramics. Among the many porous ceramics already reported via polymer pyrolysis, the literature review reveals that research on polymer derived SiC foams (PDSCFs) is limited [31].

Recently, we have developed a new replica method, to fabricate PDC foams by direct impregnation of a flexible polyurethane foam with a preceramic polymer. Accordingly, SiOC open cell foams can be produced starting from polysiloxane precursors [32].

Based on the above considerations, this work has a twofold objectives: (i) it describes an innovative and facile synthesis of SiC foams through the polymer pyrolysis route and (ii) also it reports their behavior as adsorbents towards NSAIDs and their metabolites, taken as an example of emergent organic contaminants of environmental concern belonging to the pharmaceutical class. In this regard, it should be stressed that the adsorption of these organic micropollutants has never been reported before in the literature with these kind of polymer-derived porous materials.

2. Experimental

2.1 Preparation of SiC foam

In the present work, polyurethane foam waste (PUFW) was selected as a sacrificial template material and it was collected from our University waste basket. Allylhydropolycarbosilane, SMP-10 (Starfire Systems, Schenectady, USA) was used as SiC precursor to prepare SiC foam. SMP-10 was used as received. Platinum–divinyltetramethyldisiloxane complex in xylene, with Pt content of ~2% (Sigma–Aldrich, Saint Louis, MO, USA) was used as catalyst and it was further diluted in xylene to obtain a practical solution containing 0.1 wt% of catalyst. According to the manufacturer, SMP-10 has an average molecular weight of 5000–25000 and an approximate composition of $–[SiH_2–CH_2]x–[SiH(allyl)–CH_2]y–$ in a x:y=9:1 ratio. Cross-linking of polycarbosilane can be performed via the hydrosilylation reaction of the Si–H bonds of SMP-10 with the SMP-10's allyl groups in presence of the Pt catalyst. In a typical synthesis, SMP-10 was mixed with the solvent (cyclohexane) in the presence of Pt catalyst. Cubic samples (~ 3 cm × 3 cm × 3 cm) were cut from the PUFW. The ratio of the volume of the solvent with the volume of the PUFW was kept constant to 1/5 for all the studied materials. The impregnation process was carried out manually by squeezing the flexible PUFW into the solution and releasing it, so that all the solution was sucked into the foam pores. This process was repeated several times until the foam was homogeneously wet and no solution was left in the container. The sample was prepared with polymer precursor SMP-10/PUFW weight ratio 2 and 3. The impregnated PUFW was then left to dry at room temperature for one day and then pyrolysized in a tubular furnace (Lindbergh Blue) at 2 °C/min up to 1200 °C with 2 h dwell time at the maximum temperature under nitrogen flow (200 mL/min). The resulting SiC foams were labelled PDSCFX, where "X" is the SMP-10/PUFW ratio; accordingly, foams prepared with SMP-10/PUFW ratio equal to 2 and 3, are indicated as PDSCF2 and PDSCF3, respectively.

2.2 Characterization

The shrinkage of foam samples during pyrolysis was calculated by measuring the dimensions of parallelepiped foams with a digital caliper and the weight loss associated with the polymer-to-ceramic transformation was measured with the help of microbalance. These measurements allow for calculating the bulk density (ρ_b) before and after pyrolysis. The skeletal density (ρ_s) was considered to be 3.05 g/cc for SiC [33, 34]. From the bulk and skeletal densities, the percentage of porosity, P (dimensionless) of the materials was calculated by the following equation [35]:

$$P = 100(1-\rho_b/\rho_s) \tag{1}$$

Surface morphology of the foams was examined using a scanning electron microscope (SEM, Jeol-JSM-5500). Individual cell and window sizes were measured by using Image Pro Plus software, based on several images per sample, from which average pore and window sizes were calculated.

The crystallinity of the ceramic foam was analyzed by X-ray diffraction (XRD) with a Rigaku D/Max diffractometer (Rigaku, Tokyo, Japan) in the Bragg–Brentano configuration, using Cu Kα radiation and a monochromator in the diffracted beam, in the range $2\theta = 10$–$80°$ with a $0.05°$ step and 5s acquisition time.

FT-IR spectra were collected on a Nicolet Avatar 330 Fourier transform infrared spectrometer (Thermo Electron Corporation, Waltham, MA) using KBr technique in transmission mode. An average of 64 scans with 4 cm^{-1} resolution was recorded for each specimen

Differential scanning calorimetry (DSC) analyses were performed on the PUFW and SMP-10 impregnated PUFW with a Mettler DSC30 (Switzerland) in the range of –110 to 50 °C with a heating rate of 10 °C/min, flushing with N_2 (100 mL/min). Specific surface area (SSA) of the PDSCFs was obtained at 77 K using a Micromeritics ASAP 2010 equipment (Norcross, GA, USA) with N_2 physisorption analysis (BET method).

2.3 Adsorption of NSAIDs and their metabolites

The adsorption capacity exhibited by the PDSCFs towards NSAIDs and their metabolites was evaluated by solid phase extraction, on-line coupled with liquid chromatography and tandem

mass spectrometry, following an automated analytical approach described elsewhere with full details (on-line SPE-LC-MS/MS) [36]. A liquid chromatographic system model Nexera (Shimadzu, Kyoto, Japan) and a 3200 QTrap™ mass spectrometer equipped by a Turbo V™ interface and an electrospray probe (ABSciex, Ontario, Canada) were used.

The NSAIDs and their metabolites used in this study were purchased from Sigma–Aldrich. A HCOOH/Milli-Q water 99.8/0.2 (*v/v*) solution (pH=2.50±0.05) containing all the target compounds was prepared at the final concentrations shown in **Table 1**.

Table 1 - Concentrations and amounts of target compounds used in this study. The selected compounds are: acetylsalicylic acid (ASA), salicylic acid (SAL), diclofenac (DIC), 4'-hydroxydiclofenac (4'-HYDIC), fenbufen (FEN), flurbiprofen (FLU), ketoprofen (KET), ibuprofen (IBU), 1-hydroxyibuprofen (1-HYIBU), 2-hydroxyibuprofen (2-HYIBU), naproxen (NAP) and O-desmethylnaproxen (O-DMNAP).

Compound	Concentration [ng/mL]	Amount [ng]
ASA[a]	10	500
SAL[b]	5	250
DIC[a]	2	100
4'-HYDIC[b]	2	100
FEN[a]	5	250
FLU[a]	2	100
KET[a]	2	100
IBU[a]	10	500
1-HYIBU[b]	10	500
2-HYIBU[b]	10	500
NAP[a]	5	250
O-DMNAP[b]	5	250

[a] NSAIDs; [b] NSAIDs metabolites

The PDSCF was placed in polypropylene tubes (previously tested to ensure a zero–adsorption capacity for the investigated compounds) and 50 mL of the aforementioned solution

were added in each vial. Hence, each PDSCF was in contact with amounts of target analytes reported in **Table 1**. An additional tube, devoid of the PDSCFs, was filled with 50 mL of the target compound solution and used as reference, in order to assess possible removal phenomena, different from the adsorption by PDSCFs.

The adsorption tests were performed maintaining in rotation (Reax 20, Heidolph Instruments, Schwabach, Germany) of PDSCFs and the solution under the following experimental conditions: (i) speed of 10 revolutions/minute; (ii) absence of light; (iii) room temperature (25-30 °C).

The adsorption capacity of PDSCFs towards target compounds was evaluated after 24, 48 and 72 hours of contact time, by removing 10 mL of the solution from each test tube (including the reference one) and proceeding with the on-line SPE-LC-MS/MS determination of the compounds of interest.

All aliquots collected at the different contact times (i.e. 24, 48 and 72 h) were stored at +4°C until analysis was performed and in any case not later than 24 h after the last collection. Before the on-line SPE-LC-MS/MS analysis, all collected aliquots were filtered on 0.20 µm cellulose membrane syringe filter. The evaluation of the adsorption capacity of the PDSCFs was performed through evaluation of chromatographic areas obtained with on-line SPE-LC-MS/MS analysis and their quantification by means of external calibration curves. All tests were performed in triplicate.

3. Results and discussion

3.1 Characterization of the impregnated PUFW

The impregnation process consists of wringing of PUFW several times by hand in the solution of preceramic polymer and then releasing the foam in such a way that it can absorb the solution completely within its open cells. This ensures that the solution of preceramic polymer permeates evenly throughout entire volume of the polyurethane foam network. The preceramic polymer solution can then swell the PUFW structure and when the solvent evaporates, the crosslinked preceramic polymer is retained in between the PUFW molecular structure for the subsequent pyrolysis step. In order to confirm this hypothesis, differential scanning calorimetry (DSC) analyses were performed on the PUFW and SMP-10 impregnated PUFW (**Figure 1**). Pure PUFW shows a glass transition temperature determined as the inflection point in the DSC curve

at –61°C. After the impregnation with the preceramic polymer, the glass transition temperature of PUFW shifts down to –70°C suggesting that the polyurethane chains become more mobile. This result can be rationalized assuming that, during impregnation, SMP-10 chains diffuse inside the PU network, swell the polymer and act as a plasticizer for the polyurethane.
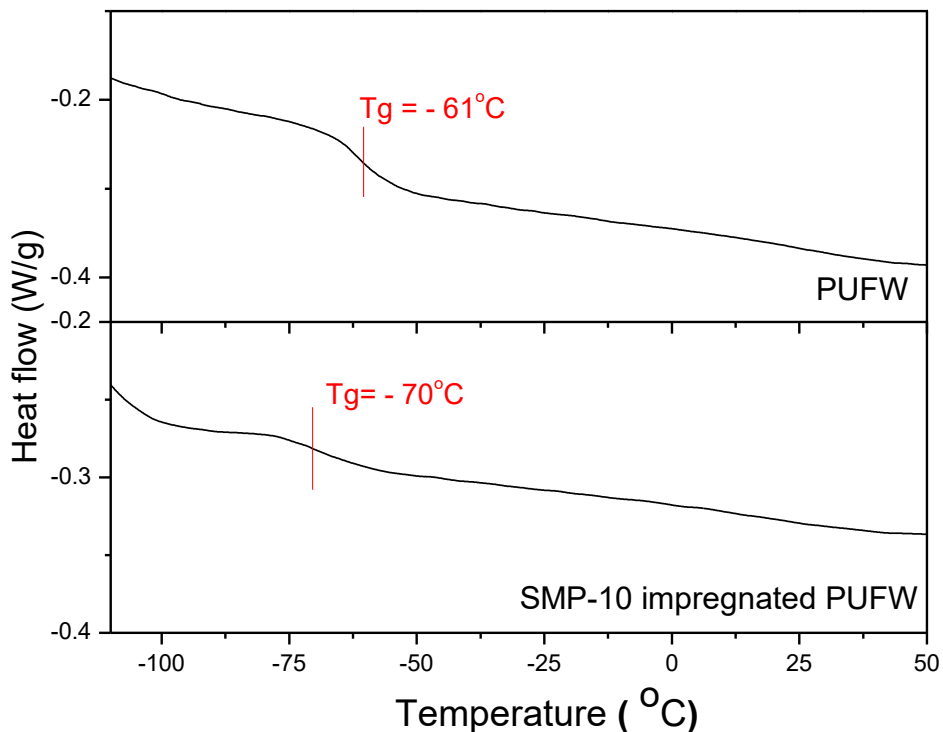

Figure 1. DSC plot of PUFW and SMP-10 impregnated PUFW.

Chemical formula of SMP-10 is reported in **Figure 2** and shows that SMP-10 contains Si–H and C=C groups which can be used, in the presence of a Pt catalyst, to crosslink the polymer via hydroxylation reaction (addition reaction) [37]. Cross-linking and impregnation of SMP-10 occur simultaneously while soaking the PUFW in the polymeric solution.
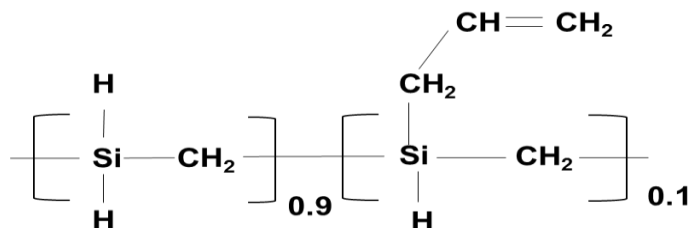

Figure 2. Chemical formulae of SMP-10.

Figure 3 shows the FTIR spectra of SPM-10, PUFW and SMP-10 impregnated foam. It is observed that peaks related to =C–H and C=C bonds are absent in the FT-IR spectrum of the dried impregnated foam suggesting an effective crosslinking at room temperature. Commercial polyurethane foam belongs to two main types: ester– and ether–based. The absorption band at 1725 cm^{-1} corresponds to C=O groups while the peak at 1124 cm^{-1} is assigned to C–O bonds. Based on the relative intensity of these two bands showing a much stronger intensity of the C–O compared to the C=O vibration, we can conclude that the used PUFW is an ether–based type since in the ester–based polyurethane the number of C=O and C–O moieties is comparable while in the ether-based polymers the C–O groups of the ether moiety are predominant.
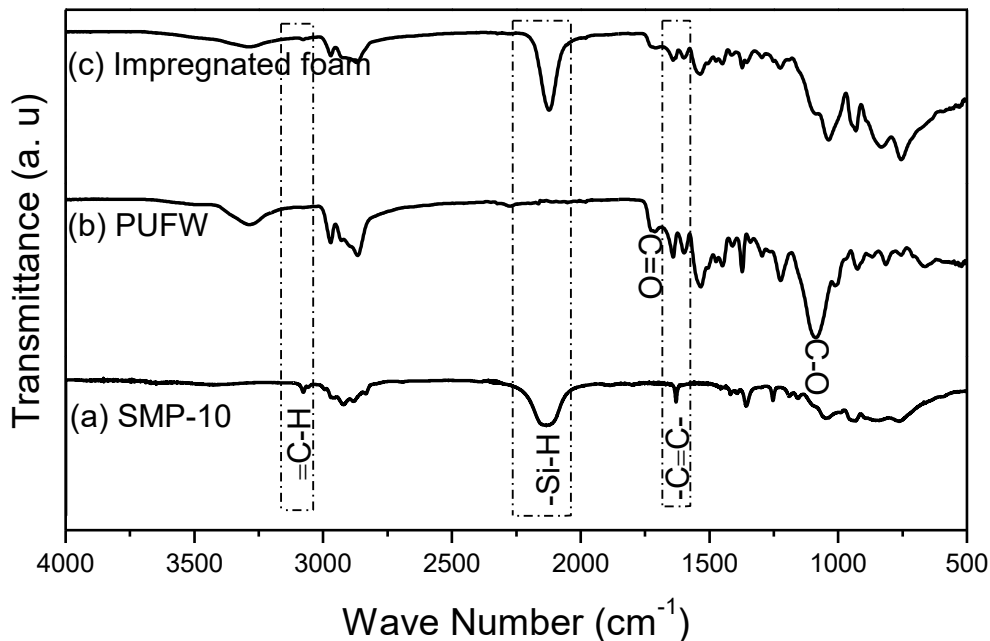
Figure 3. FT-IR spectra of SMP-10, PUFW and SMP-10 impregnated foam.

3.2 Characterization of the ceramic foams

The polymer-to-ceramic conversion of the PDSCF2 and PDSCF3 samples result into a linear and volume shrinkage of ~30% and ~60%. This result suggests that the shrinkage during pyrolysis is controlled by the shrinkage of the polycarbosilane, which is, indeed, close to 30% [38]. The mass loss is ~50% and 40%, respectively for PDSCF2 and PDSCF3. The bulk density is 0.11 g/cc (porosity 96%) and 0.16 g/cc (porosity 95%) for PDSCF2 and PDSCF3, respectively.

The successful conversion of the impregnated PUFW foams into the ceramic SiC foams can be appreciated from the SEM pictures reported in **Figure 4** and **5**. **Figure 4** shows SEM images of the initial PUFW. From these images, the average cell, window and strut sizes were found to be 724, 266 and 77 µm, respectively. PUFW exhibits cells of near hexagonal configuration that are interconnected by other cells. The struts of pores are regular and smooth.
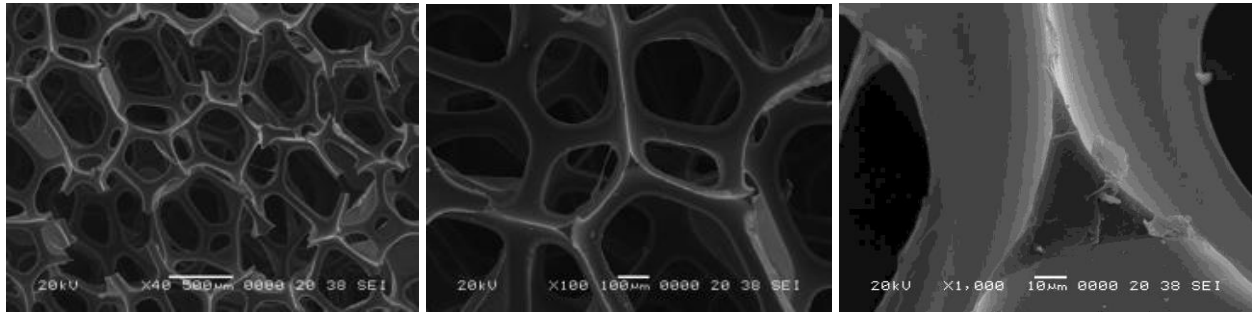

Figure 4. SEM images of PUFW at various magnifications.

Figure 5 shows the microstructure of the resultant PDSCF2. As expected, the morphology of the PDSCF2 is a perfect replica of the PUFW, however with a smaller cell (485 µm), window (165 µm) and strut size (60 µm). SEM pictures made at higher magnification are also given in **Figure 5** and as expected, they show that the struts are dense, without any central cavity. In this regard, it should be noted that the formation of dense struts is not trivial, since, for the conventional ceramic foams made with the replica techniques starting from ceramic suspension, hollow struts are formed. Indeed in the conventional process, the ceramic slip coats the PU foams and when the polymeric foam burns out it leaves behind a central cavity. In our process, the preceramic polymer diffuses in between the PU chain and impregnates homogeneously the polyurethane foams struts as it was shown by the DSC study. Accordingly, during pyrolysis the PU decomposes while the preceramic polymer transforms into the ceramic materials leading to the formation of dense struts.
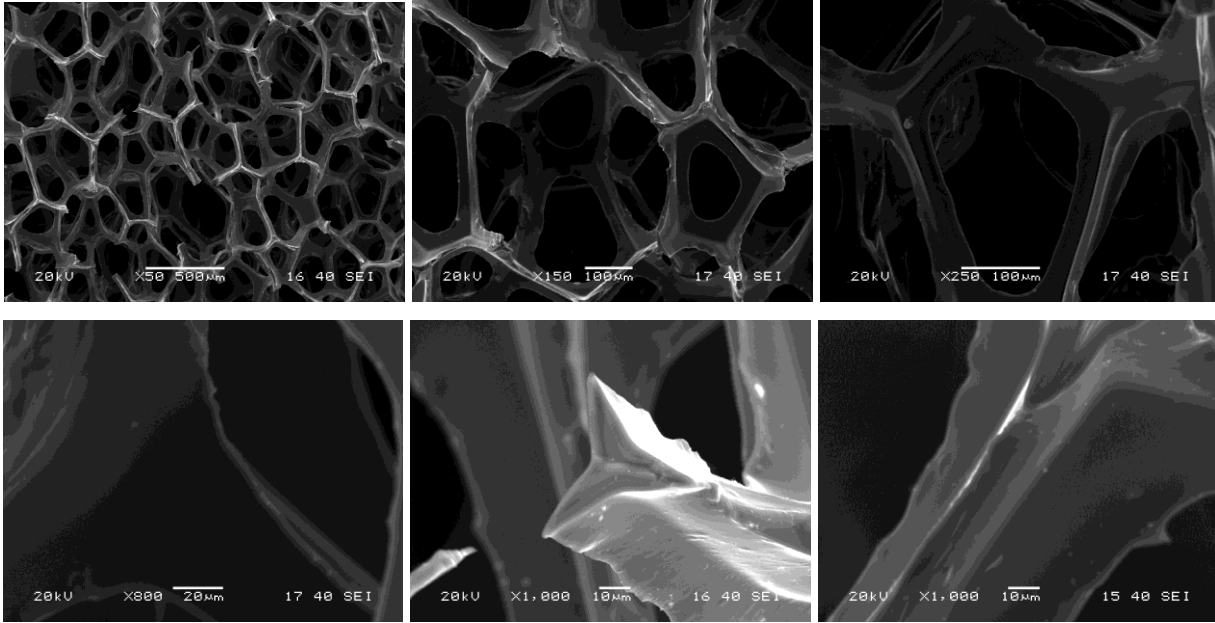
Figure 5. SEM images of the resultant PDSCF2 at various magnifications.

The structure of the ceramic foams has been investigated by FT-IR and XRD. The Infra-red spectrum (**Figure 6a**) shows a main peak at 810 cm^{-1} assigned to the Si-C stretching vibration which confirms the successful formation of the silicon carbide foam. The small absorption at 1090 cm^{-1} (Si-O stretching) suggests that, during pyrolysis, some oxygen has been incorporated in the foam, either from O_2 impurities present in the furnace or through a reaction with the decomposition products of the PUFW. Finally, the broad peak in the range 3600–3400 cm^{-1} and the one at 1637 cm^{-1} indicate the presence of silanol and adsorbed water, respectively. **Figure 6b** reports the XRD pattern of PDSCF pyrolized at 1200°C, which is characterized by broad diffraction peaks at 35°, 60° and 72°, corresponding to (111), (220) and (311) of nanocrystalline cubic silicon carbide (β–SiC).
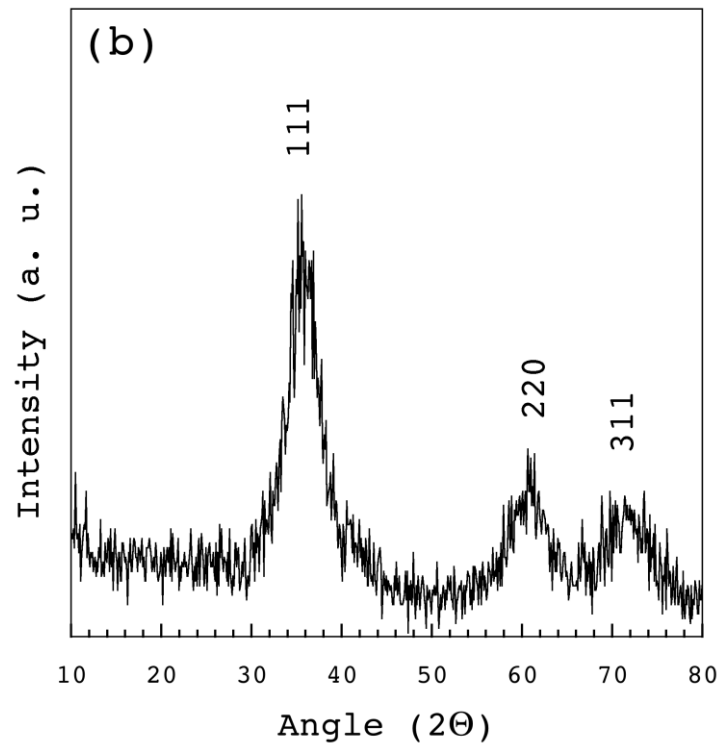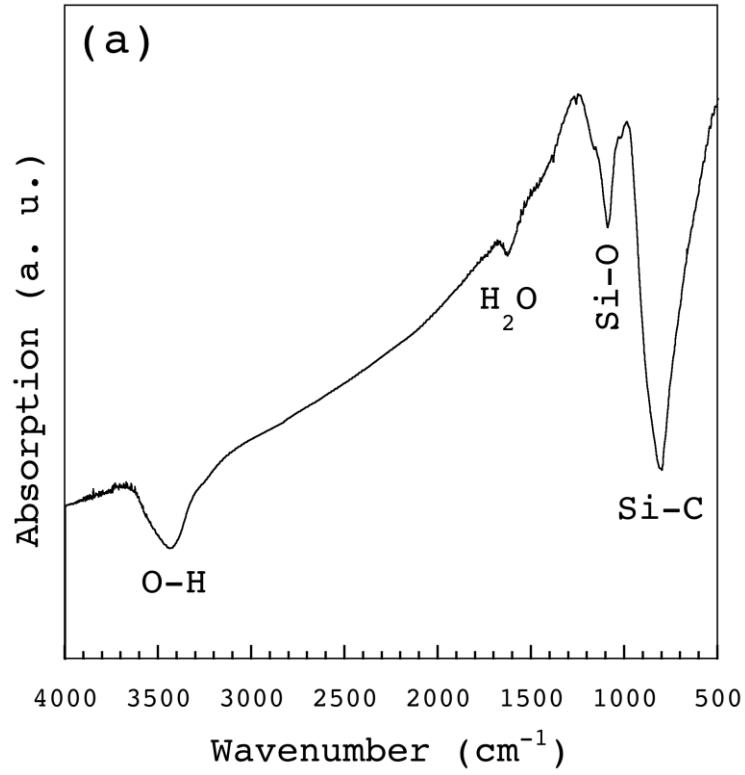
Figure 6. (a) FT-IR spectrum and (b) XRD pattern of PDSCF.

3.3 Adsorption study

Figure 7 illustrates the trend of the adsorption percentage, as a function of contact time (24, 48 and 72 h) between the solution of target compounds and PDSCF2 (**Figure 7A**) or PDSCF3 (**Figure 7B**). The results showed that the adsorption increases with increasing the contact time; moreover, the differences in adsorption percentages among the tested contact times were quite similar, thus suggesting that adsorption phenomenon is governed by a slow kinetic. According to the structural characterization of the PDSCFs (See FT-IR spectrum in **Figure 3**), the studied materials have silanol groups on the surface. Moreover polymer derived ceramics have, in general, free carbon in their structure and most probably, given the "black" color of the studied foams, this is also true in the present case. Therefore, being the target compounds characterized by the presence of various moieties, such as aromatic rings, carboxylic and phenolic groups, etc., hydrogen bonds, π-π interactions or van der Waals forces are expected to be involved in the adsorption process, according to the different structure of the various investigated compounds.
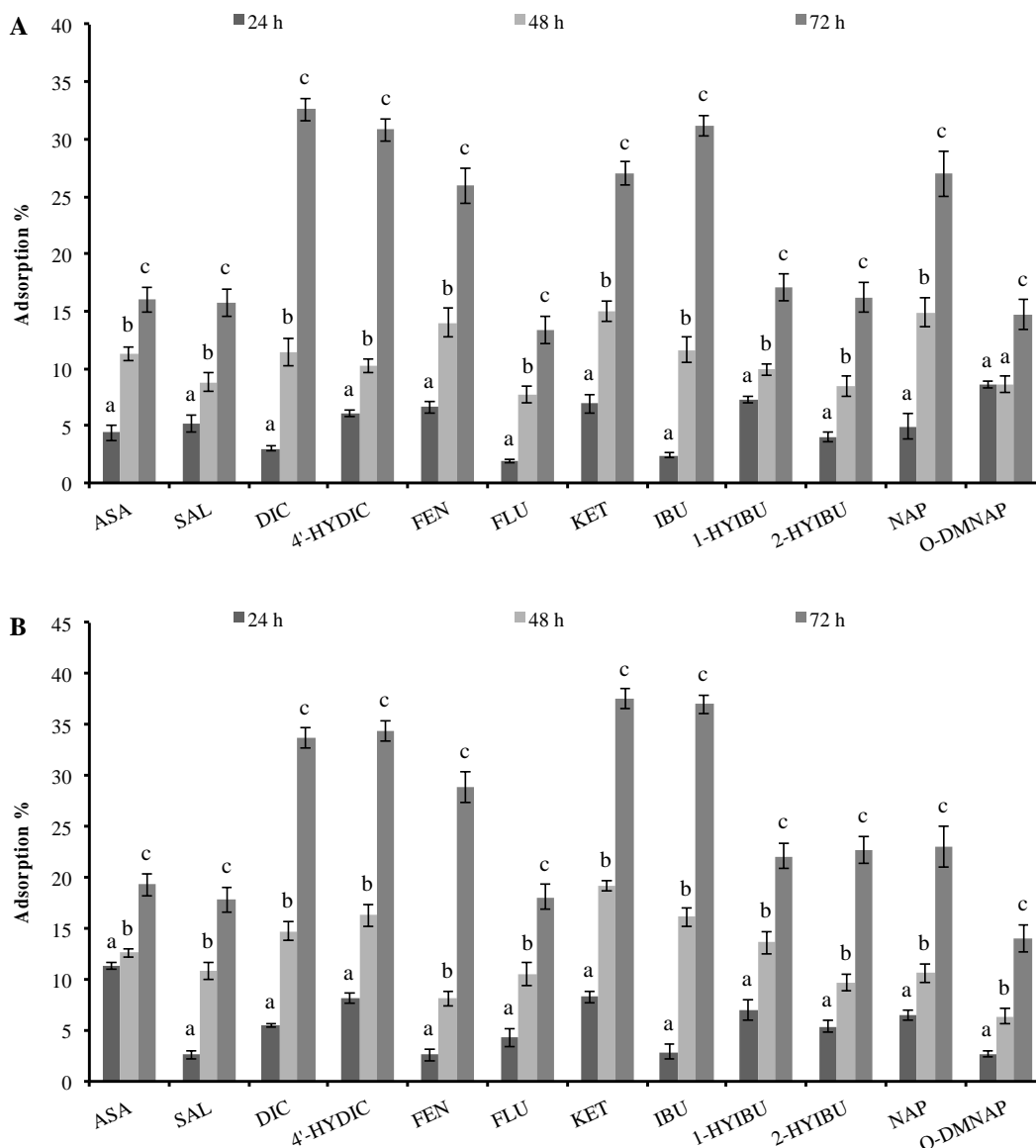
Figure. 7 – Adsorption percentages determined for PDSCF2 (A) and PDSCF3 (B) towards target compounds after 24, 48 and 72 h of contact time.

Since PDSCF used in the various adsorption tests were characterized by different mass and volume, in order to compare the adsorption values obtained with different foam samples, it is necessary to normalize the results as a function of the volume and mass of each specific foam sample. Accordingly, **Table 2** illustrates the adsorption values, normalized to ng/cc and ng/g, for each investigated compound, for both PDSCF2 and PDSCF3, after 72 h of contact time.

Table 2 – Adsorption values normalized to ng/cc and ng/g for each investigated compound for both PDSCF2 and PDSCF3, after 72 h of contact time.

Compound	Normalized adsorption [ng/cc]		Normalized adsorption [ng/g]	
	PDSCF2	PDSCF3	PDSCF2	PDSCF3
ASA	97.0	57.2	2169	1025
SAL	91.7	58.5	1062	472
DIC	461.8	313.8	882	358
4'-HYDIC	254.8	187.4	834	365
FEN	240.9	192.5	1751	765
FLU	80.3	63.8	360	192
KET	39.6	30.7	730	399
IBU	192.6	122.3	4199	1961
1-HYIBU	201.0	97.8	2317	1171
2-HYIBU	109.5	59.5	2190	1203
NAP	238.5	164.0	1828	611
O-DMNAP	116.8	75.5	995	372

From the **Table 2**, it can be concluded that PDSCF2 showed better performance for adsorbing NSAIDs compared to PDSCF3. For example, 1 g of PDSCF2 can adsorb about 4200 ng of Ibruprofen whereas 1 g of PDCF3 can adsorb only approximately 2000 ng. In order to rationalize this result, it is worth recalling that: (i) the struts are dense and the interaction between the analyte and the foam occurs through the external surface of the struts; (ii) the difference in the two foams relies in the amount of SMP-10 used for their synthesis, being for the PDSCF3 higher compared to PDSCF2. As previously described, the use of higher amount of SMP-10 leads to the formation of PDSCFs with higher density (0.16 vs 0.11 g/cc) and slightly lower porosity (95 vs 96%). In these types of open cell foams, the foam density can increase by increasing the average thickness of the struts and accordingly, the specific surface area, either expressed as $\dfrac{m^2}{g_{of\ foam}}$ or as $\dfrac{m^2}{m^3_{of\ foam}}$ decreases by increasing the density of the foam. Taken all

together, these results imply that the surface of the struts, which is available in 1 gram (or in 1 cc) of foams to adsorb the analytes, is higher in the PDSCF2 compared to PDSCF3. Comparing the normalized adsorption values expressed as ng/g, we can see that PDSCF2 adsorbs roughly twice as much as the PDSCF3. This results can be rationalized using the specific surface area (SSA). Accordingly, the SSA of PDSCF2 (0.31 m^2/g) is two times higher than PDSCF3 (0.13 m^2/g) suggesting that the NSAIDs adsorption capacity is governed by SiC foam surface. Considering the total adsorption capacity for the two foams (19317 ng/g for the PDSCF2 and 8894 ng/g for the PDSCF3), specific adsorption capacity value close to 70 μg/m^2 is obtained, which is in line with the reported literature for other types of porous adsorbent [39].

4. Conclusions

Open cell SiC foams have been successful processed via a new replica method using a polyurethane foam waste and a preceramic polymer. The preceramic polymer can homogeneously swell the polyurethane structure and during pyrolysis leads to the formation of dense struts, contrary to the conventional replica method, which uses a ceramic slurry, results into hollow struts. With this process, the density of the ceramic foam can be controlled by the initial amount of preceramic polymer used for the impregnation of the PUFW. Accordingly polymer-derived SiC foams with density of 0.11 and 0.16 g/cc had been prepared and the liquid-phase adsorption of NSAIDs and their metabolites had been studied for the first time. The results showed that the adsorption increases with increasing the contact time; and that adsorption phenomenon is governed by a slow kinetic. From this study, it can be suggested that SiC foam materials can be applied in the adsorptive removal of NSAIDs and their metabolites in contaminated water.

References

[1]   I. Maijó, F. Borrull, C. Aguilar, M. Calull, Determination of Anti-Inflammatory Drugs in River Water by Sweeping-Micellar Electrokinetic Capillary Chromatography, J. Liq. Chro. Rel. Tech. 35 (2012) 2134–2147.

[2]   N. Migowska, M. Caban, P. Stepnowski, J. Kumirska, Simultaneous Analysis of Non-Steroidal Anti-Inflammatory Drugs and Estrogenic Hormones in Water and Wastewater Samples Using Gas Chromatography-Mass Spectrometry and Gas Chromatography with Electron Capture Detection, Sci. Tot. Environ. 441 (2012) 77–88.

[3]   M. Villar Navarro, M. Ramos Payan, R. Fernández-Torres, M.A. Bello-López, M.C. Mochon, A.G. Pérez, Capillary Electrophoresis Determination of Nonsteroidal Anti-Inflammatory Drugs in Wastewater Using Hollow Fiber Liquid-Phase Microextraction, Electrophoresis, 32 (2011) 2107–2113.

[4]   Report on "Pharmaceutical Pollution in the Environment: Issues for Australia, New Zealand and Pacific Island countries", www.ntn.org.au

[5]   B. Halling-Sorensen, S. Nors Nielsen, P.F. Lanzky, F. Ingerslev, H.C. Holten Liitzhofl, S.E. Jorgensen, Occurrence, Fate and Effects of Pharmaceutical Substances in the Environment – A Review, Chemosphere, 36 (1998) 357–393.

[6]   R. Gothwal, T. Shashidhar, Antibiotic Pollution in the Environment: A Review. CLEAN – Soil, Air, Water, 43 (2015) 479–489.

[7]   E. Larsson, S. al-Hamimi, J.Å. Jönsson, Behaviour of nonsteroidal anti-inflammatory drugs and eight of their metabolites during wastewater treatment studied by hollow fibre liquid phase microextraction and liquid chromatography mass spectrometry, Sci. Total Environ. 485–486 (2014) 300–308.

[8]   J. Radjenovic´, M. Petrovic´, D. Barcelo´, Fate and distribution of pharmaceuticals in wastewater and sewage sludge of the conventional activated sludge (CAS) and advanced membrane bioreactor (MBR) treatment, Water Research, 43 (2009) 831–841.

[9]   D. Rossini, L. Ciofi, C. Ancillotti, L. Checchini, M.C. Bruzzoniti, L. Rivoira, D. Fibbi, S. Orlandini, M. Del Bubba, Innovative combination of QuEChERS extraction with on-line solid-phase extract purification and pre-concentration, followed by liquid chromatography-tandem mass spectrometry for the determination of non-steroidal anti-

inflammatory drugs and their metabolites in sewage sludge, Analytica Chimica Acta (2016), http://dx.doi.org/10.1016/j.aca.2016.06.023.

[10]   D.W. Kolpin, E.T. Furlong, M.T. Meyer, E.M. Thurman, S.D. Zaugg, L.B. Barber, H.T. Buxton, Pharmaceuticals, hormones, and other organic wastewater contaminants in US streams, 1999–2000: a national reconnaissance, Environ. Sci. Technol. 36 (2002) 1202–1211.

[11]   S.M. Rivera-Jiménez, S. Méndez-González, A. Hernández-Maldonado, Metal, (M = Co^{2+}, Ni^{2+}, and Cu^{2+}) grafted mesoporous SBA-15: Effect of transition metal incorporation and pH conditions on the adsorption of Naproxen from water, Micropo. Mesopo. Mater. 132 (2010) 470–479.

[12]   G.R. Boyd, H. Reemtsma, D.A. Grimm, S. Mitra, Pharmaceuticals and personal care products (PPCPs) in surface and treated waters of Louisiana, USA and Ontario Canada, Sci. Total Environ. 311 (2003) 135–149.

[13]   A. Joss, S. Zabczynski, A. Göbel, B. Hoffmannc, D. Löffler, C.S. McArdell, T.A. Ternes, A. Thomsen, H. Siegrist, Biological degradation of pharmaceuticals in municipal wastewater treatment: proposing a classification scheme, Water Res. 40 (2006) 1686–1696.

[14]   C. Zwiener, F.H. Frimmel, Short-term tests with a pilot sewage plant and biofilm reactors for the biological degradation of the pharmaceutical compounds clofibric acid, ibuprofen, and diclofenac, Sci. Total Environ. 309 (2003) 201–211.

[15]   H.-R. Busar, T. Poiger, M.D. Müller, Occurrence and fate of the pharmaceutical drug diclofenac in surface waters: rapid photodegradation in a lake. Environ. Sci. Technol. 32 (1998) 3449–3556.

[16]   M. Grassi, G. Kaykioglu, V. Belgiorno, G. Lofrano, Removal of Emerging Contaminants from Water and Wastewater by Adsorption Process, in: G. Lofrano (ed.), Emerging Compounds Removal from Wastewater SpringerBriefs in Green Chemistry for Sustainability, 2012, pp. 15–37.

[17]   V. Matamoros, C. Arias, H. Brix, J.M. Bayon, Preliminary screening of small scale domestic wastewater treatment systems for removal of pharmaceutical and personal care products, Water Res. 43 (2009) 55–62.

[18]   T. Nagano, K. Sato, T. Saitoh, Y. Iwamoto, Gas Permeation Properties of Amorphous SiC Membranes Synthesized from Polycarbosilane without Oxygen–Curing Process, J. Ceram. Soc. Jpn. 114 (2006) 533–538.

[19]   H. Suda, H. Yamauchi, Y. Uchimaru, I. Fujiwara, K. Haraya, Preparation and gas permeation properties of silicon carbide-based inorganic membranes for hydrogen separation, Desalination, 193 (2006) 252–255.

[20]   M. Fukushima, Y. Zhou, H. Miyazaki, Y. Yoshizawa, K. Hirao, Y. Iwamoto, S. Yamazaki, T. Nagano, Microstructural Characterization of Porous Silicon Carbide Membrane Support With and Without Alumina Additive, J. Am. Ceram. Soc. 89 (2006) 1523–1529.

[21]   J.S. Lee, S.H. Lee, S.C. Choi, Improvement of porous silicon carbide filters by growth of silicon carbide nanowires using a modified carbothermal reduction process, J. Alloys Compd. 467 (2009) 543–549.

[22]   Y. Liu, O. Ersen, C. Meny, F. Luck, C. Pham-Huu, Fischer–Tropsch Reaction on a Thermally Conductive and Reusable Silicon Carbide Support, ChemSusChem., **7** (2014) 1228–1239.

[23]   G. Karagiannakis, C.C. Agrafiotis, C. Pagkoura, A.G. Konstandopoulos, D. Thomey, L. de Oliveira, M. Roeb, C. Sattler, Hydrogen production via sulfur-based thermochemical cycles: Part 3: Durability and post-characterization of silicon carbide honeycomb substrates coated with metal oxide–based candidate catalysts for the sulfuric acid decomposition step. Int. J. Hydrogen Energy, 37 (2012) 8190–8203.

[24]   P. Krawiec, S. Kaskel, Thermal stability of high surface area silicon carbide materials. J. Solid State Chem. 179 (2006) 2281–2289.

[25]   D. Galsterer, N. Travitzky, T. Wolff, P. Greil, Microstructure and Properties of SiC Honeycomb Structures. Adv. Eng. Mater. 10 (2008) 1134–1140.

[26]   U.F. Vogt, L. Gyorfy, A. Herzog, T. Graule, G. Plesch, Macroporous silicon carbide foams for porous burner applications and catalyst supports, J. Phys. Chem. Solids, 68 (2007) 1234–1238.

[27]   S. Wood, A.T. Harris, Porous burners for lean-burn applications, Prog. Energy Combust. Sci. 34 (2008) 667–684.

[28]   A. Ortona, S. Pusterla, P. Fino, F.R.A. Mach, A. Delgado, S. Biamino, Aging of reticulated Si-SiC foams in porous burners, Adv. Appl. Ceram., 109 (2010) 246–251.

[29]   C.C. Agrafiotis, I. Mavroidis, A.G. Konstandopoulos, B. Hoffschmidt, P. Stobbe, M. Romero, V. Fernandez-Quero, Evaluation of porous silicon carbide monolithic honeycombs as volumetric receivers/collectors of concentrated solar radiation, Sol. Energy Mater. Sol. Cells, 91 (2007) 474–488.

[30]   M. Fukushima, Microstructural control of macroporous silicon carbide, J. Ceram. Soc. Jpn. 121 (2013) 162–168.

[31]   M. Fukushima, P. Colombo, Silicon carbide-based foams from direct blowing of polycarbosilane, J. Europ. Ceram Soc., 32 (2012) 503–510.

[32]   G.D. Soraru, R. Campostrini, A.A. Ejigu, E. Zera and P. Jana, Processing and characterization of polymer derived SiOC foam with hierarchical porosity by HF etching, J. Ceram. Soc Jpn., (2016), accepted.

[33]   P. Colombo, Conventional and novel processing methods for cellular ceramics, Philos. Trans. Royal Soc. A: Math. Phys. Eng. Sci., 364 (2006) 109–24.

[34]   P. Colombo, G. Mera, R. Riedel, G.D. Soraru, Polymer-Derived Ceramics: 40 Years of Research and Innovation in Advanced Ceramics, J. Am. Ceram. Soc., 93 (2010) 1805–1837.

[35]   P. Jana, V. Ganesan, Synthesis, characterization and radionuclide (^{137}Cs) trapping properties of a carbon foam, Carbon, 47 (2009) 3001–3009.

[36]   L. Ciofi, D. Fibbi, U. Chiuminatto, E. Coppini, L. Checchini, M. Del Bubba, Fully-automated on-line solid phase extraction coupled to high-performance liquid chromatography–tandem mass spectrometric analysis at sub-ng/L levels of selected estrogens in surface water and wastewater, J. Chromatogr. A, 1283 (2013) 53–61.

[37]   G.D. Sorarù, F. Dalcanale, R. Campostrini, A. Gaston, Y. Blum, S. Carturan, P.R. Aravind, Novel polysiloxane and polycarbosilane aerogels via hydrosilylation of preceramic polymers, J. Mater. Chem. 22 (2012) 7676–7680.

[38]   F. Dalcanale, J. Grossenbacher, G. Blugan, M. R. Gullo, A. Lauria, J. Brugger, H. Tevaearai, T. Graule, M. Niederberger, J. Kuebler, Influence of carbon enrichment on electrical conductivity and processing of polycarbosilane derived ceramic for MEMS applications, J. Europ. Ceram. Soc. 34 (2014) 3559–3570.

[39]   G. Simões dos Reis, C.H. Sampaio, E. C. Lima, M. Wilhelm, Preparation of novel adsorbents based on combinations of polysiloxanes and sewage sludge to remove pharmaceuticals from aqueous solutions, Colloids and Surfaces A: Physicochem. Eng. Aspects 497 (2016) 304–315.

[40]   **Figure captions**

Figure 1. DSC plot of PUFW and SMP-10 impregnated PUFW.

Figure 2. Chemical formulae of SMP-10.

Figure 3. FT-IR spectra of SMP-10, PUFW and SMP-10 impregnated foam.

Figure 4. SEM images of PUFW at various magnifications.

Figure 5. SEM images of the resultant PDSCF2 at various magnifications.

Figure 6. (a) FT-IR spectrum and (b) XRD pattern of PDSCF.

Figure. 7 Adsorption percentages determined for (A) PDSCF2 and (B) PDSCF3 towards target compounds after 24, 48 and 72 h of contact time.

Table captions

Table 1 – Concentrations and amounts of target compounds used in this study. The selected compounds are: Acetylsalicylic acid (ASA), Salicylic acid (SAL), Diclofenac (DIC), 4'-Hydroxydicolenac (4'-HYDIC), Fenbufen (FEN), Flurbiprofen (FLU), Ketoprofen (KET), Ibuprofen (IBU), 1-Hydroxyibuprofen (1-HYIBU), 2-Hydroxyibuprofen (2-HYIBU), Naproxen (NAP) and O-Desmethylnaproxen (O-DMNAP).

Table 2 – Adsorption values normalized to ng/cc and ng/g for each investigated compound for both PDSCF2 and PDSCF3, after 72 h of contact time.